Engineering 2015, 1(3): 351–360
DOI 10.15302/J-ENG-2015081

Research
Medical Instrumentation—Article

A Confocal Endoscope for Cellular Imaging

Jiafu Wang[1,2], Min Yang[3], Li Yang[1,2], Yun Zhang[1,2], Jing Yuan[1,2], Qian Liu[1,2], Xiaohua Hou[3], Ling Fu[1,2]*

ABSTRACT Since its inception, endoscopy has aimed to establish an immediate diagnosis that is virtually consistent with a histologic diagnosis. In the past decade, confocal laser scanning microscopy has been brought into endoscopy, thus enabling *in vivo* microscopic tissue visualization with a magnification and resolution comparable to that obtained with the *ex vivo* microscopy of histological specimens. The major challenge in the development of instrumentation lies in the miniaturization of a fiber-optic probe for microscopic imaging with micron-scale resolution. Here, we present the design and construction of a confocal endoscope based on a fiber bundle with 1.4-μm lateral resolution and 8-frames per second (fps) imaging speed. The fiber-optic probe has a diameter of 2.6 mm that is compatible with the biopsy channel of a conventional endoscope. The prototype of a confocal endoscope has been used to observe epithelial cells of the gastrointestinal tracts of mice and will be further demonstrated in clinical trials. In addition, the confocal endoscope can be used for translational studies of epithelial function in order to monitor how molecules work and how cells interact in their natural environment.

KEYWORDS cellular resolution, confocal endoscopy, optical biopsy

1 Introduction

Cancer is a major disease affecting human health. According to the *World Cancer Report 2014*, approximately 14 million new cancer cases and 8.2 million cases of cancer-related deaths occurred in 2012, and the estimated number of annual cancer cases will increase to 22 million in the next 20 years [1]. The early diagnosis and treatment of cancer are critical for improving quality of life and reducing treatment costs. Considering that 85% of tumors originate from epithelial cells, techniques for detecting the disease at the cellular level are urgently needed. Traditional methods for cancer diagnosis are generally based on screening for a serum-specific antigen or other tumor markers with limited specificity and sensitivity [2]. Over the past decade, many imaging techniques, such as computed tomography, magnetic resonance imaging, ultrasound imaging, and positron emission tomography, have undergone great improvements in sensitivity and resolution. Nevertheless, their resolution is still limited to the submillimeter level.

According to the Annual Cancer Registration of China, cancer associated with the gastrointestinal tract accounted for more than 22% of all cases in 2012. Therefore, a high-resolution detection method is critical for clinical applications, especially for the early diagnosis of cancer in the gastrointestinal tract. Endoscopy is a routine method used for gastrointestinal tract diagnosis. With the development of technology, gastrointestinal endoscopy has passed through three phases: the rigid endoscope era (1805–1932); the semi-flexible endoscope era (1932–1957); and the fiber-optic era (1957–present) [3]. The fiber-optic endoscope, known as the flexible endoscope, was first assembled in 1957 and developed rapidly thereafter [4, 5]. Recently, gastrointestinal endoscopy took a big step forward with the combination of fiber-optic and confocal technologies.

Chromoendoscopy (CE) is another well-known endoscopy technology [6, 7]. In CE, staining technology improves the intensity of signals from tissues, leading to higher specificity and lesion characterization compared with colonoscopy and white-light endoscopy [7, 8]. However, the process of staining makes CE more time-consuming than other endoscopic techniques.

In recent years, a new type of endoscope, the confocal endoscope, has emerged with the use of laser scanning confocal imaging technology and a fluorescent indicator. The confocal endoscopy can characterize cell morphology in a way that is highly consistent with biopsy pathology images, enabling doctors to accurately determine *in situ* whether tissue is cancerous, precancerous, or healthy, with minimal discomfort to patients [9]. Currently, the confocal endoscope is the only endoscopic instrument that is able to conduct cellular imaging with micron-scale resolution. This instrument represents a leap forward in the history of endoscope development. Clini-

[1] Britton Chance Center for Biomedical Photonics, Wuhan National Laboratory for Optoelectronics, Huazhong University of Science and Technology, Wuhan 430074, China; [2] MoE Key Laboratory for Biomedical Photonics, Department of Biomedical Engineering, Huazhong University of Science and Technology, Wuhan 430074, China; [3] Division of Gastroenterology, Union Hospital, Tongji Medical College, Huazhong University of Science and Technology, Wuhan 430074, China
* Correspondence author. E-mail: lfu@mail.hust.edu.cn
Received 5 August 2015; received in revised form 6 September 2015; accepted 10 September 2015

cal studies have shown that confocal endoscopy has great clinical value and potential in the diagnosis of early colon cancer lesions, ulcerative colitis, Barrett's esophagus, gastroesophageal reflux, non-erosive reflux disease, and other diseases of the digestive tract [10].

In this paper, we briefly introduce the concept of confocal endoscopy with a particular focus on its key components and technology. Next, we present a prototype of confocal endoscope that was developed to be compatible with conventional endoscopes for gastroenterology. The important components of this prototype are described, and its performance, including field-of-view (FOV) and resolution, is characterized. As a demonstration of the prototype, the imaging results of the large intestine of a mouse are presented. The prototype of the confocal endoscope has passed the medical device supervision and testing conducted by the China Food and Drug Administration and is set to begin clinical trials.

2 Background of confocal endoscopy

Endoscopy is the touchstone of gastrointestinal disease diagnostics. With the aid of the endoscopic technique, we can see places invisible to the naked eye from the mouth to the anus, including the stomach, duodenum, small intestine, and colorectum, as well as organs next to the digestive tract such as the pancreas and biliary tract [11]. With the development of this technology, several typical endoscopic techniques have become widely used in hospital settings, such as conventional endoscopy and narrow band imaging (NBI). Because it uses reflected light, conventional endoscopy has a low resolution, almost the same as that of the naked eye, and can only be used to observe macrostructure, with no cellular information. Figure 1(a) presents an image of gastric intestinal metaplasia using conventional endoscopy (EG-590WZ, Fujinon, Tokyo, Japan). The image shows that the mucosa of the gastric antrum is rough, but provides no other useful information. Although NBI, which uses blue and green wavelengths to enhance the detail of certain aspects of the surface of the mucosa, can detect the vascular morphology, it is still unable to identify tissue at a cellular level. Figure 1(b) shows the tissue imaged using NBI (CV-290/CLV-290, Olympus, Tokyo, Japan); the gland ducts are ovate, and there is a light blue crest (LBC) in part of the image. Figure 1(c) shows an image acquired with a confocal endoscope (Cellvizio, Mauna Kea Technologies (MKT), Paris, France), including several black goblet cells scattered in the epithelial cells of the gastric antrum glands. These goblet cells can be observed clearly. Figure 1(d) shows a histologic image of the gastric intestinal metaplasia; there are many vacuole-like intestinal epithelial cells in the gland ducts of the gastric antrum. These images demonstrate that confocal endoscopy is the only endoscopic technique that can operate at the cellular level *in vivo* in real time. In a study of pathological diagnoses of biopsies taken from observed sites to serve as gold standards, 87 patients were examined by NBI, CE, and confocal endoscopy for atrophic gastritis. The results showed that confocal endoscopy had a higher sensitivity, specificity, and accuracy than CE and NBI [12].

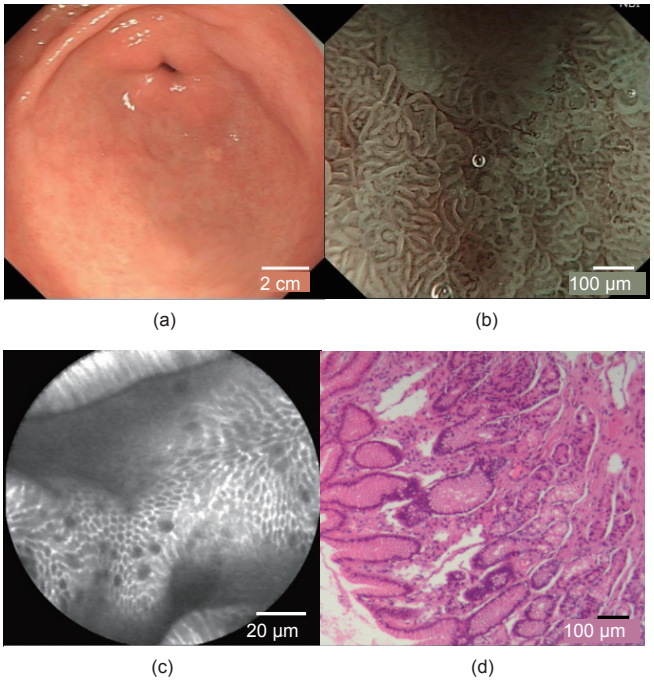

Figure 1. Images of gastric intestinal metaplasia (GIM, gastric antrum) from different devices. (a) An image taken using conventional endoscopy, with no microstructures visible; (b) imaged by NBI, vascular structures can be seen but no cells can be observed; (c) imaged by confocal endoscopy, epithelial cells and the goblet cells are visible; (d) a corresponding histologic image.

The advent of confocal endoscopy has changed the diagnostic methods used with traditional endoscopes. First, the ability to distinguish cells can help to identify subtle and flat mucosal lesions. Second, confocal endoscopy can produce real-time images *in vivo* without damage to the tissue. Confocal endoscopy is an endoscopic ultrahigh magnification technique that enables microscopic analysis of the mucosa during an ongoing endoscopy, making it possible for gastroenterologists to diagnose diseases at an early stage in the gastrointestinal tract. In addition, confocal endoscopy can be used to target biopsies in large or diffuse lesions (i.e., "smart biopsies") and to guide and survey endoscopic resection [13]. Although biopsy is still the gold standard for diagnostics, it is not superior to confocal endoscopy when all factors are taken into consideration. The *in vivo* histological imaging enabled by confocal endoscopy is a targeted method that could reduce diagnosis time by reducing the blindness of sampling. Therefore, we believe that this new direction will greatly facilitate and promote the development of endoscopic technology.

3 Key components and technology

3.1 Laser scanning confocal microscopy

Confocal microscopy, a practical technique that can greatly improve the signal-to-noise ratio and axial resolution by reducing stray light signals from the sample above or below the focal plane by employing a pinhole, has rapidly developed since its invention in 1957 by Marvin Minsky. Figure 2 shows the principle of confocal microscopy.

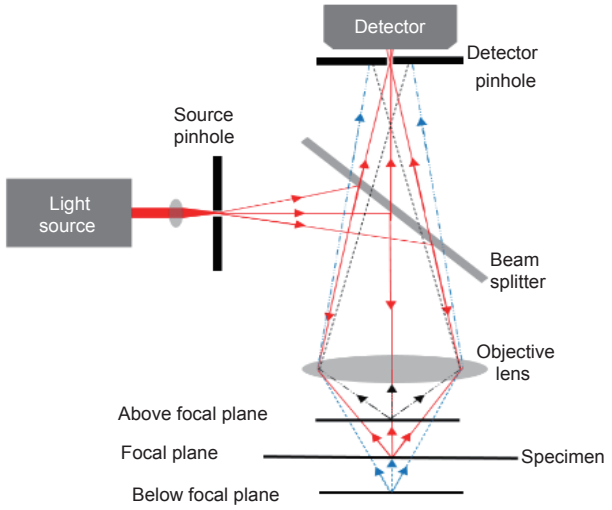

Figure 2. Schematic diagram of a confocal microscopy. The detector pinhole, point light source at the source pinhole, and illuminated spot in the specimen are conjugate to each other. The detector pinhole in front of the detector can reject stray light from above (the light in black) or below (the light in blue) the focal plane.

A point light source is formed by converging the beam from the laser with a lens. Light from the source is reflected by a beam splitter and then focused by the objective. The specimen is illuminated and emits fluorescence. The fluorescence with a longer wavelength will be collected by the objective lens and will pass through the beam splitter to the detector. A pinhole that is conjugated to the point light source is placed before the detector to reject excited signals from out-of-focus regions; only the signal from the focal point can be collected.

Compared with conventional wide-field microscopic imaging, confocal microscopy provides great advantages, such as its high axial resolution due to the use of a pinhole. A confocal microscopy can also detect the sample at different depths, known as optical sectioning, which has never been realized before. The optical sectioning capability makes confocal microscopy well-suited for imaging thick tissue *in vivo* without the need for tissue slicing before experiments, as is required for conventional histological detection. This capability is also practical in clinical applications for qualitative analyses of diseases.

3.2 Optical fiber and fiber bundle

Although confocal microscopy has been met with enthusiasm by biologists throughout its development, the cumbersome objective lens has been the primary obstacle to its clinical application from the outset. In 1991, a confocal endoscope, with a single-mode fiber (SMF) used to substitute for the confocal pinhole, first performed *in vivo* clinical imaging [14–16]. The optical fiber was less frequently used in confocal laser scanning microscopy but developed quickly for telecommunications applications.

As shown in Figure 3(a), the simplest optical fiber comprises a core of glass with a high refractive index (RI) of n_1 and a cladding of a different glass with a lower RI of n_2 surrounding the core. The light traveling through the fiber core is confined by the effect called total internal reflection. The optical fiber, with its particular advantage of flexibility, makes the confocal microscopy accessible to the human body without losing its optical sectioning and high-resolution properties.

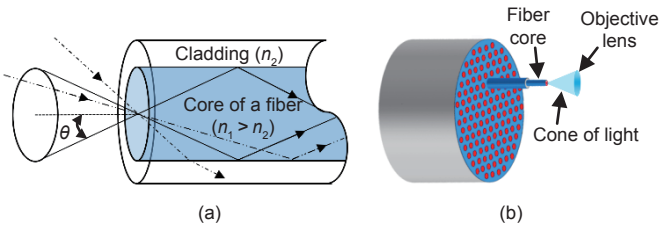

Figure 3. Coupling of light to the fiber and optical fiber bundle. (a) Only the light in the core can be transmitted with no leakage; (b) a fiber bundle contains many fibers, ranging from less than 2000 to as many as 100 000.

In 2006, a confocal endoscope employing an SMF was introduced for use in clinical applications. In addition to transmitting the excitation light and collecting fluorescence from the tissue, the single optical fiber (or every optical fiber in a bundle) serves as a pinhole for confocal imaging by reducing the scattered light. The subsequent commercial probe-based confocal endoscope uses a fiber bundle instead of an SMF. As shown in Figure 3(b), a fiber bundle is made up of a large number of fibers. Only light in the core can be transmitted effectively. The number of fibers and the space between adjacent fibers determine the FOV and the resolution, respectively [17]. The fiber bundle can be inserted into the biopsy channel of a conventional endoscope due to its small size and has become increasingly important in the development of the endoscopic armamentarium. At their highest resolution, both of these types of endoscopes can distinguish cells in different tissues in the human body in real time, a feat that has not been achieved by other endoscopes [18–20].

3.3 Micro-objective lens

The miniature objective is one of the most important components of a confocal endoscope. The miniature objective is used to focus the excitation light onto the tissue and collect emission light from the tissue. The resolution and FOV of confocal endoscopy are determined by the numerical aperture (NA) and the magnification of the miniature objective. The small size of the lens system enables access into the human body through the biopsy channel of a gastroendoscope. Thus, a prerequisite for qualified imaging in confocal endoscopy is to use a high-NA miniature objective of a small size.

Gradient-index (GRIN) lenses are preferred due to their small outer diameters. A high-NA GRIN lens assembled with a low-NA GRIN lens is usually used for microscopic endoscopy [21, 22]. However, it is difficult for a GRIN lens system to correct aberrations such as chromatic aberration and curvature of field. Therefore, a GRIN lens system is less suitable for fluorescence confocal endoscopy.

To improve imaging performance, a custom-designed lens system is a preferred solution. However, there are two major challenges for the design of a miniature objective. First, because the fabrication and assembly of lenses with small outer diameters are complex processes with limited techniques, the lens design should consider both the optical parameters and

the manufacturing process. Second, the miniature objective should have a short length to enable flexibility and accessibility to internal organs. With a shorter length than that of a commercial microscope objective, a miniature objective must use a smaller number of optical elements to correct aberrations. Consequently, creating a suitable balance of design, fabrication, and assembly is critical for developing a miniature objective.

Table 1 summarizes the specifications of micro-objectives used in confocal endoscopy. Custom-designed miniature objectives with all-glass spherical lenses have been achieved for both reflectance and fluorescence confocal endoscopy [23, 24]. However, the structure of an all-glass spherical lens results in more optical elements in the miniature objective, making the assembly procedure complicated. Aspheric plastic lenses combined with glass spherical lenses can reduce the number of optical elements for reflectance confocal endoscopy [25, 26]. A miniature objective with a diffraction-limited capability for fluorescence confocal endoscopy within the wavelength range of 452–623 nm can be designed with six aspheric plastic lenses [27].

The design of a high-NA miniature objective with a small number of optical elements remains a challenge. At present, a miniature objective composed of both aspheric and spherical lenses is easier to produce. With the development of new technologies for fabrication and assembly, the degree of freedom in the design of miniature objectives will be increased, enabling improved imaging quality.

3.4 Fiber scanning devices

A compact scanning device is essential in confocal endoscopy because confocal microscopy is a point-to-point laser scanning technology. In general, the miniature scanning mechanism for fiber endoscopy can be classified into two categories. The first category of mechanism acts to manipulate the illumination of the laser beam like a traditional galvanometer mirror. A two-dimensional microelectromechanical system (MEMS) mirror, which is inserted between a fiber end and a miniature objective, serves as a light manipulator [28]. This approach benefits from the small size of the mirror and low power consumption, and MEMS has shown potential for miniaturization. However, this solution has not been widely adopted, due to its complexity and high price.

Instead of scanning the laser beam, the second category of mechanism acts to deflect the illumination fiber directly. In this method, the illumination beam emerging through the fiber core is collimated and focused by micro-optics (e.g., GRIN lenses), which means that any movement of the fiber end translates to a small lateral displacement of the focusing spot. By deflecting the fiber tip, two-dimensional scanning can be achieved at the focus plane.

Due to its high sensitivity, fast response speed, and low cost, a piezoelectric element has gradually become a promising choice for deflecting the fiber tip. In particular, a piezoelectric bender can vibrate in correspondence with the driving voltage due to the inverse piezoelectric effect. A nonresonant piezolever fiber scanner was developed to measure calcium signals in individual neurons of the neocortex at a 15 Hz frame rate in freely behaving rats [29]. The FOV was approximately 260 μm in diameter, and images had 64 × 64 pixels when operating at 10.9 Hz. The scanner consists of four piezoelectric benders, a scanning fiber, and two thinner fibers serving as a hinge. Benefiting from the lever principle, the tiny deflection induced by the piezoelectric bender can be translated into a large fiber cantilever displacement [30]. The lever comprises two components: a free-fiber cantilever and a small component between the cross point and the fiber anchor. When driven by the saw-like signal at the fast axis, together with the ramp signal at the slow axis, a raster-like scanning pattern is produced. This mechanism also permits vector scanning and random access scanning. However, a nonresonant piezolever fiber scanner usually requires a large piezoelectric bender driven by a high voltage to afford sufficient fiber-tip deflection.

Fortunately, taking advantage of resonance amplification, a miniature resonant piezoelectric fiber scanner can provide an adequate scanning range with a low driving voltage. In addition, a resonant scanner usually has a high frame rate due to its higher resonance frequency. A resonant piezoelectric fiber scanner typically consists of a piezoelectric tube and a fiber [31]. The fiber cantilever vibrates in two orthogonal directions so that essentially no cross-talk exists. A spiral scanning pattern can easily be achieved by driving vibrations in orthogonal directions with a 90° phase shift [32]. The front piece is 32 mm in length, and the outer diameter is 2 mm. When operated at a resonance frequency of 1.4 kHz, the imaging frame rate, the frequency (rate) at which a monitor displays, is 2.7 frames per second (fps) and the FOV is approximately 110 μm. Table 2 shows different miniature scanning mechanism features.

Our group has developed a resonant fiber-optic piezoelectric scanner (RFPS) using four piezoelectric elements arranged as a square tube, which is efficient to fabricate and

Table 1. Specifications of micro-objective lenses.

Parameter	Knittel et al. [21]	Rouse et al. [23]	Liang et al. [24]	Chidley et al. [25]	Kester et al. [26]	Kyrish et al. [27]
Number of elements	2	9	8	5	3	6
Outer diameter (mm)	1	4	7	7	4	2.1
Length (mm)	7.8	13	20.4	17.5	10	10
Confocal endoscopy	Fluorescence	Fluorescence	Reflectance	Reflectance	Reflectance	Fluorescence
NA at tissue	0.5	0.46	1.0	1.0	1.0	0.55
FOV (μm)	280	450	250	250	250	360
Lateral resolution (μm)	3.1	1.8	0.93	0.65	0.65	4.4

Table 2. Miniature scanning mechanism features.

Type	MEMS [28, 33]	Nonresonant [30]	Resonant [31]
Schematic diagram	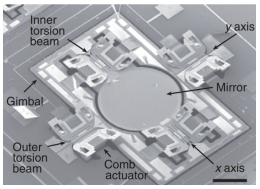	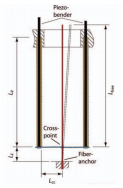	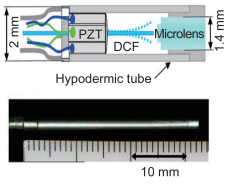
Geometry size	20 mm × 19 mm × 11 mm	2 mm × 10 mm	ϕ2 mm × 25 mm
Driving voltage	60 V/150 V	124 V	140 V
Frequency / frame rate	1.08 kHz & 0.56 kHz/1–15 fps	790 Hz/10.9 fps	1.4 kHz/2.7 fps
FOV	295 μm × 100 μm	260 μm	110 μm
Features	Small size, low power consumption; complexity, high price	Random access scanning; large size, high voltage	High resonant frequency; lacking vector scanning

drive [34]. By using a coupled-field model based on a finite element method, the scanning properties of the scanner, including vibration mode, resonance frequency, and scanning range, can be numerically studied for general-purpose designs. The piezoelectric patches are 16 mm × 1.2 mm × 0.2 mm in size and the cantilever is a piece of SMF that is 16 mm in length and 125 μm in diameter. Driven by a low voltage of 10 V, the maximal scanning ranges of the cantilever tip in two directions appear at the frequencies of 384 Hz and 370 Hz, corresponding to scanning ranges of 1.671 mm and 1.893 mm, respectively. Different pixels correspond to different imaging frame rates, and the typical imaging frame rate is 2 fps. Images can be obtained by spiral scanning, as shown in Figure 4(a) [34]. Moreover, the RFPS can be designed to achieve raster scanning by producing differently ordered resonances in two orthogonal directions, as shown in Figure 4(b) [35]. The square pattern is obtained if the drive voltages are 3 Hz/20 V and 879 Hz/154 V for the frame scanning and line scanning, respectively.

4 A fiber-optic confocal endoscope

4.1 System configuration

An intravital optical imaging method with minimal or no invasiveness has been the goal of gastroenterologists since the origin of medical devices. In the gastrointestinal tract, biopsy has been the gold standard. However, a biopsy process is time-consuming and unable to realize optical imaging in real time. In addition, the bulky objective lens of a traditional optical imaging system has inhibited clinical application. The fiber-bundle-based confocal endoscope, combining a confocal laser scanning microscope and a fiber bundle, provides an effective solution to this problem that retains the advantages described above.

We developed a confocal endoscope with high resolution by using the confocal laser scanning technique, which is critical to achieving high resolution. Figure 5 diagrams the schematic of our fiber-bundle-based confocal endoscope system. Figure 6 shows the confocal endoscope system. A 488 nm laser is used as a light source because the fluorescences of common dyes such as fluorescein and acriflavine hydrochloride are easily excited at this wavelength [36, 37]. After being emitted from the laser (OBIS 488-50, Coherent, Santa Clara, CA, USA), the beam is expanded to satisfy the incident condition of the objective lens (20×/0.50, Olympus, Tokyo, Japan) and is then reflected by a 488 nm cutoff dichroic mirror (DM, Semrock, Rochester, NY, USA). An *XY* scanner module, composed of a counter rotation scanner mirror and a galvanometer mirror, scans the laser light. The imaging speed is 4 fps with 1024 × 1024 pixels, and 8 fps with 512 × 512 pixels. The beam is then relayed by a pair of lenses and incident on the back aperture of the objective lens, which will couple the laser beam into the proximal end of a fiber bundle (FIGH-30-650S, Fujikura, Tokyo, Japan). All the fibers in the bundle are used to transmit the excitation laser as well as the fluorescence light. A micro-objective lens that directly contacts the sample is adhered at the other end of the fiber. The fluorescence, generated at the focal point with a longer wavelength, is collected by the micro-objective lens. The fluorescence passes through the dichroic mirror and a filter (FF02-525/40,

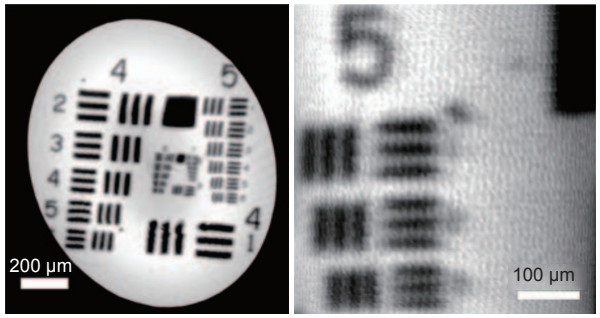

Figure 4. Images of a USAF 1951 resolution target. (a) Spiral scanning, with the scale bar at 200 μm [34]; (b) raster scanning, with the scale bar at 100 μm [35].

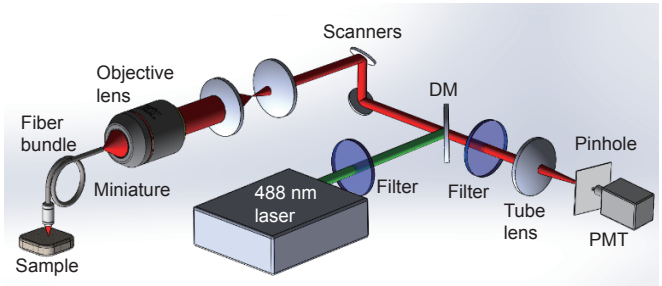

Figure 5. Schematic diagram of the confocal endoscope. DM: dichroic mirror; PMT: photomultiplier tube.

Semrock, Rochester, NY, USA) and is then collected by a tube lens. At the focus of the tube lens, a pinhole, which is conjugated to the focus of the objective lens on the proximal end of the fiber bundle, is used to block stray light. Finally, a photomultiplier tube (R3896, Hamamastu, Shizuoka Pref., Japan) is used to detect the signal.

A confocal endoscope prototype with a high resolution was constructed, as shown in Figure 6(a). The prototype consists of a portable scanning unit, a foot switch to control the laser and record the data, a computer for data processing and image display, and a probe. The portable scanning unit integrates the optical elements and electronics. The pluggable probe, a combination of an optical fiber bundle and a micro-objective lens, is independent from the scanning unit, as shown in Figure 6(b).

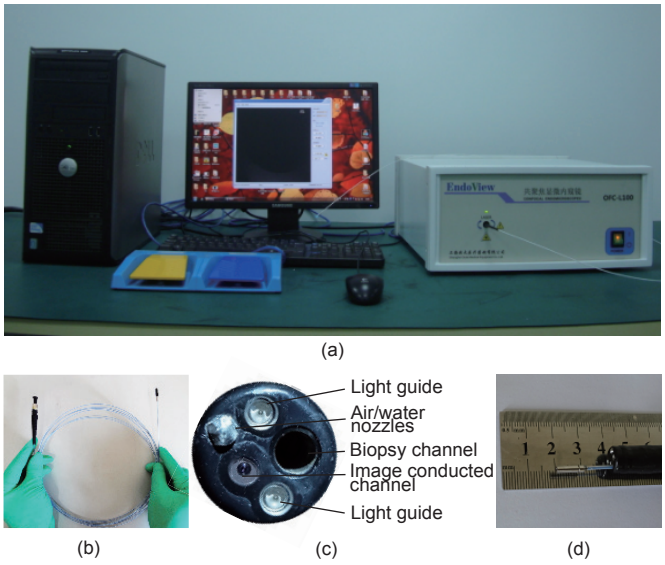

Figure 6. Confocal endoscope system. (a) Confocal endoscope prototype; (b) probe of confocal endoscope; (c) end face of a conventional endoscope; (d) probe passing through a conventional endoscope.

4.2 Miniaturized fiber probe for gastroenterology

Figure 6(b) and Figure 6(c) present the optical probe of our confocal endoscope and a probe of a conventional endoscope (GIF-XQ40, Olympus, Tokyo, Japan). The optical fiber probe is the critical component of the confocal endoscope. The micro-objective lens in the optical fiber bundle directly determines the imaging resolution. To further improve the lateral resolution of this confocal endoscope, we designed a micro-objective lens with a diameter of 2.6 mm. As shown in Figure 6(d), the probe is compatible with the biopsy channel of a conventional endoscope, so there is no need for a special endoscope. In addition to size, aberration must be taken into consideration in the lens design. We constructed a micro-objective lens with simultaneous correction of spherical aberration, chromatic aberration, and field curvature.

Currently, there are only two companies—Pentax/Hoya (Tokyo, Japan) and MKT—that can manufacture confocal endoscopes for gastroenterology *in vivo* with cellular resolution. The greatest difference between the EC-3870CIk (produced by Pentax/Hoya) and the Cellvizio (produced by MKT) exists in the scanning position; the former scans distally, whereas the latter scans proximally. In the distal scanning design, the single fiber is scanned by an electromagnetically driven scanning mechanism, but the miniaturization of the scanner remains a problem for compatibility with conventional endoscopes and many other applications [38]. However, with the use of a proximal scanning device and a fiber bundle, the size of the scanner is no longer a problem. Instead, various probes can be designed for different purposes. For this reason, probes for different applications have emerged in recent years, such as the S series for surface imaging, the M series for high-resolution imaging, and the Z series for depth imaging [39]. The confocal endoscope with a proximal scanning design is compatible with conventional endoscopes. Compatibility is critical because incompatibility leads to an additional cost for a specific endoscope, which would be prohibitive.

4.3 Image-processing algorithm

Compared with conventional endoscopy, confocal endoscopy enables non-invasive and cellular-resolution imaging in real time. In confocal endoscopy, the coherent optical fiber bundle plays a vital role in conducting the excitation light and the fluorescence signal. The fiber bundle is composed of a large number of single fibers, with each fiber made up of a high-transmittance core and low-transmittance cladding, resulting in a honeycomb pattern, which is detrimental to imaging resolution, in the original fluorescence image. Therefore, it is essential to eliminate the honeycomb pattern without a deterioration of image quality. Based on previous studies of the honeycomb pattern elimination problem, three approaches are introduced here to achieve high-resolution image recovery.

In the first approach, termed the spatial filtering algorithm, the honeycomb pattern is regarded as a disturbance. To remove this disturbance, a mean filter is applied to the effective image region, which was previously determined to avoid signal broadening, in order to suppress the noise; then histogram equalization is utilized to enhance image contrast. Finally, the honeycomb pattern is removed by employing Gaussian filtering.

The second method is the frequency domain filtering algorithm. First, two-dimensional fast Fourier transform is used to acquire the frequency domain information of the image. Because the honeycomb pattern is arranged pseudo-periodically in the spatial domain with a high frequency, its frequency domain information mainly corresponds to high-frequency components. Next, a specifically designed Gaussian low-pass filter is sufficient to remove the frequency domain information of the honeycomb pattern. Finally, a recovered image can be attained by applying the inverse fast Fourier transform to the filtered frequency domain information.

The triangulation reconstruction algorithm is the third choice. A honeycomb pattern in the image reflects the lateral structure of the fiber bundle [40]. Because cladding hinders the sampling of information located at the cladding corresponding region in the sample plane, this algorithm regards pixels that correspond to the center of the fiber core as correctly sampled pixels, deemed "center pixels." The aim of this algorithm is to interpolate the image based on the center

pixels. The triangulation reconstruction algorithm comprises three steps. The first step is calculating the center pixels, which can be achieved with local extrema searching and additional filtering. The second step is applying Delaunay triangulation to triangulate the set of calculated center pixels [41]. The third step is linearly interpolating every non-center pixel based on the gray values of the vertexes of the covering triangle that was obtained in the second step.

An image of a *Convallaria* stem acquired by confocal endoscope is shown in Figure 7(a), in which the honeycomb pattern is obvious. Figure 7(b) shows the processed image produced by the spatial filtering algorithm. The honeycomb problem is alleviated, and the structure of the *Convallaria* stem is clear. Because of the weighted averaging or smoothing filter used, the signal level and the image contrast are decreased compared with the original image, and the image is also blurred. The advantage of this algorithm is its high speed: A speed of 8 fps is achievable in the confocal endoscope system using this approach. Figure 7(c) shows the result of the frequency domain filtering algorithm. In this figure, the structure of the *Convallaria* stem is complete and undistorted; however, with the elimination of the honeycomb pattern, the edge information in the original image—information that is mainly contained in the high-frequency components—is also lost, resulting in blurring. The decrease in signal level and image contrast is a problem for both the spatial filtering algorithm and the frequency domain filtering algorithm, but both algorithms are fast. Figure 7(d) shows the result of the triangulation reconstruction algorithm. The honeycomb problem is greatly alleviated compared with the results from the previous two algorithms, and the signal level and image contrast are increased as well. However, this algorithm is relatively slow and cannot meet the real-time requirement for confocal endoscopy. Table 3 presents a comparison of these three algorithms.

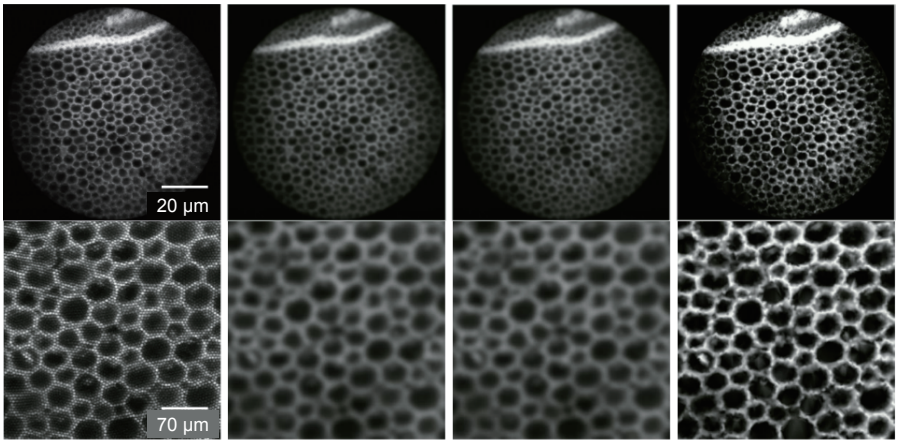

Figure 7. A comparison of the honeycomb pattern elimination methods. (a) Confocal image of the *Convallaria* stem; (b) processed by spatial filtering algorithm; (c) processed by frequency domain filtering algorithm; (d) processed by triangulation reconstruction algorithm.

4.4 Performance of our confocal endoscope system

The fiber bundle we used had a coating diameter of 750 μm and an active image circle diameter of only 620 μm. The FOV is halved with the use of a homemade micro-objective lens. As shown in Figure 8(a), only the areas that contain fibers are bright, and the honeycomb structures are visible. With the *XY* scanners, the coupling of light from the objective lens to each optical fiber at the proximal end of fiber bundle realizes the point-to-point transmission. As a fiber bundle is used to conduct the light, the end face must exactly coincide with the focal plane of the objective lens. If this happens, every fiber in the bundle can be imaged clearly, as shown in Figure 8(b). If the end face of the fiber bundle is in front of or behind the focal plane, we obtain only blurred images. In addition to these two cases, a more complex situation occurs when the end of a fiber is not vertical to the optic axis.

As shown in Figure 9(a), when a grating (80 L/MM, Edmund, Barrington, NJ, USA) with a fluorescent reagent was placed in front of the probe of the confocal endoscope, the stripes of the grating could be seen clearly. In the image, 25 stripes are present that correspond to an FOV of approximately 310 μm. As in microscopy imaging, a wide field is always an advantage. The FOV of our confocal endoscope is sufficiently wide to observe tissue.

For the fiber-bundle-based confocal endoscope, the distance between adjacent fiber cores determines the resolution. In order to evaluate the resolution of our system, a standard 1951 US Air Force (USAF) target, shown in Figure 9(b), was imaged. Because the target is not a fluorescent sample, the fluorescein solution was dropped on the front of the target. As shown in Figure 9(c), the minimally resolved bars are group 8 and element 4 in the blue oval, corresponding to a resolution of 1.4 μm. This resolution is high enough to distinguish the cells on the surface of the mucosa in the digestive tract of humans and mice. Table 4 compares the main parameters of our system with those of commercial confocal endoscopes. Com-

Table 3. A comparison of the honeycomb pattern elimination methods.

Algorithm	Spatial domain	Frequency domain	Triangulation
Contrast	Normal	Normal	Excellent
Details	Normal	Normal	Excellent
Speed	>> 8 fps	>> 8 fps	Slow

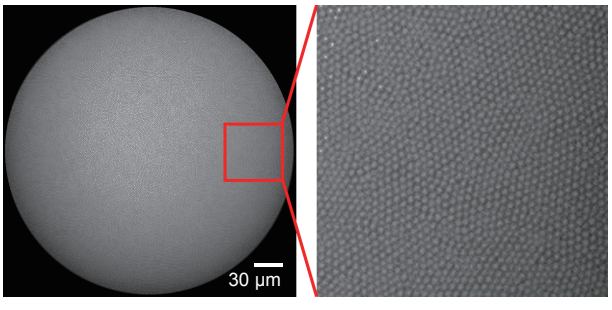

Figure 8. The end face of the optical fiber bundle. (a) The end face of the optical fiber bundle; (b) enlarged detail of the red rectangle in (a), all the fibers in the red rectangle can be seen.

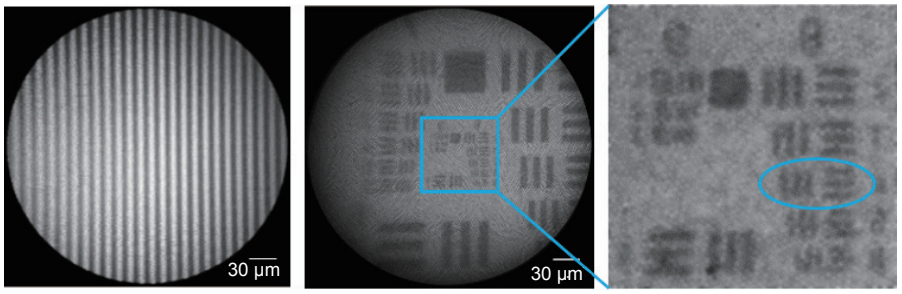

(a) (b) (c)

Figure 9. Parameter test using a grating and the USAF target. (a) Imaging of the grating with a standard of 80 L·mm^{-1}; (b) image of the USAF target used to determine spatial resolution of the confocal endoscope system; (c) enlarged detail of the blue rectangle in (b).

Table 4. A comparison of the main parameters of our homemade portable confocal endoscope and commercial confocal endoscopes.

Probes		Size of probe (mm)	Lateral resolution (μm)	FOV (μm × μm)	Working distance (μm)
Homemade	S-500	0.8	2.8	620	0
	U-240	2.6	1.4	310	150
Pentax/Hoya	ISC-1000	12.8	0.7	475	250
MKT	S-650	0.65	3.3	600	0
	UltraMinio	2.6	1.4	240	60
	Minio/30	4.2	1.4	240	30
	Mini-Z	0.91	3.5	325	50 or 70

paring our homemade system with the Pentax/Hoya and MKT systems, the lateral resolution of the Pentax/Hoya system is slightly higher, but its endoscope diameter is large. Both our system and the MKT systems use probe-based methodology to enable a diversity of probes for versatile clinical applications.

5 Cellular imaging

5.1 Experimental methods

C57BL/6 mice weighing ~ 20 g were purchased from the Zhongnan Hospital of Wuhan University (Hubei, China) and maintained under specific-pathogen-free conditions. All experiments were performed according to the animal experiment guidelines of the Animal Experimentation Ethics Committee of Huazhong University of Science and Technology (Hubei, China). To improve the contrast of signals from tissues, acriflavine hydrochloride, a commonly used contrast agent, was used to stain the surface of mucosa [37]. Acriflavine hydrochloride is an effective dye with no serious adverse reactions [38]. This dye immediately combines with the deoxyribonucleic acid (DNA) and ribonucleic acid (RNA) of the cell nuclei after topical application. The C57BL/6 mice were anaesthetized by intraperitoneal injection of urethane (90 μL/10 g) and then dissected to expose the large intestine. Subsequently, the large intestine was excised and stained with 0.1% (w/v) acriflavine hydrochloride. Finally, the probe of the confocal endoscope system was placed in direct contact with the mucosa of the large intestine in order to perform the imaging. The excitation wavelength is 488 nm, and the spectral wavelength of image detection ranges from 505 nm to 545 nm.

5.2 Imaging results

Here, we observed the large intestine of C57BL/6 mice stained by acriflavine hydrochloride using our confocal endoscope system. Descending colon mucosa and rectal mucosa were clearly observed, as shown in Figure 10(a). Crypts, which are typical structures of the colon, were round or oval and were regularly distributed. In the FOV, there were approximately 5–12 uniform mucous secreting crypts [9, 42]. In addition, because acriflavine hydrochloride stained the tissue surface, the epithelial cells were observed to be closely distributed around the crypts. For the rectal mucosa, similar structures were observed, as shown in Figure 10(b).

Only the surface of mucosa can be dyed by acriflavine hydrochloride. However, the subsurface can also be stained by acriflavine hydrochloride, as shown in Figure 11, although the lamina propria, located approximately 50 μm below the mucosal surface, cannot. The surface of the mucosa can be seen, as shown in Figure 11(a), and the fluorescence from the subsurface can also be detected, as

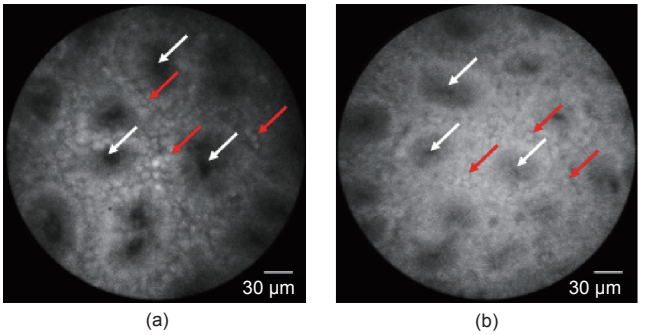

(a) (b)

Figure 10. Confocal images of descending colon mucosa and rectal mucosa of mice after topical application of 0.1% acriflavine hydrochloride. (a) Descending colon mucosa; the superficial cells have been strongly stained and closely distributed around the crypts; (b) rectal mucosa; the red arrows indicate the columnar epithelial cells and the white arrows indicate crypts.

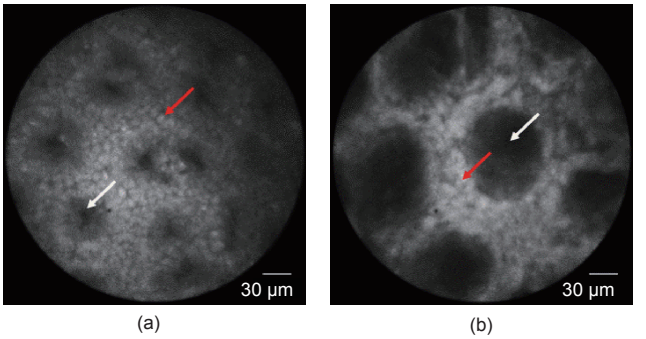

(a) (b)

Figure 11. Confocal images of the descending colon mucosa of mice after topical application of 0.1% acriflavine hydrochloride. (a) The superficial cells have been strongly stained; (b) the subsurface is stained as well, but the epithelial cells can hardly be distinguished. The red arrows indicate epithelial cells and the white arrows indicate crypts.

shown in Figure 11(b). This ability to image at various depths shows the optical sectioning ability of this confocal endoscope system.

Furthermore, we found that the structures were not exactly the same throughout the colon. In some areas, the epithelial cells centralized on the surface of the mucosa and there were no goblet cells, as shown in Figure 12(a). In other areas, we found extracellular matrix or goblet cells dispersed around the crypts, depicted in Figure 12(b). The goblet cells are black due to the mucin inside.

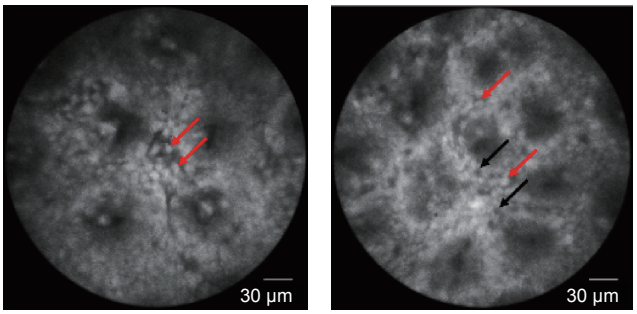

Figure 12. Confocal images of the descending colon mucosa and the ascending colon of mice after topical application of 0.1% acriflavine hydrochloride. (a) The descending colon mucosa; the epithelial cells can be observed; (b) the ascending colon, with the goblet cells dispersed around the crypts. The red arrows indicate the epithelial cells and the black arrows indicate goblet cells.

6 Discussion and perspective

The confocal endoscope with a miniaturized probe enables the *in vivo* and real-time imaging of different tissues, cells, molecules, and even bacteria under healthy and pathological conditions [43, 44]. Many studies have confirmed that the confocal endoscopy has a high diagnostic accuracy. Confocal endoscopy is not intended to replace histopathology, but rather to guide biopsies to regions of interest based on microstructures (i.e., smart biopsies) [20]. This technique is becoming an important tool for clinical and research applications.

However, there are still some limitations in confocal endoscopy. The imaging depth of the endoscope limits our observation to the surface of tissues such as intestinal epithelial cells (IECs) and intraepithelial papillary capillary loops (IPCLs). The cells and tissues under IECs, such as those of the enteric nervous system (ENS) and immunocytes in the lamina propria layer, which are important for intestinal motility, sensation, and immunity, cannot be observed [45]. This limitation could be overcome in the next generation of confocal systems, which might be considerably improved if combined with infrared technologies. Meanwhile, in order to take advantage of the sectioning ability of confocal microscopic imaging, axial scanning methods should also be explored in the future in order to shift the focal plane into tissue for 3D visualization with a depth of around 100 μm.

The confocal endoscope system that is commonly used in the clinic has only one excitation wavelength, restricting the fluorescent dyes that can be used to sodium fluorescein, acriflavine hydrochloride, and the dyes or radiolabeling that are combined with specific antibodies [46]. This restriction limits the use of many dyes with cellular or molecular specificity or with low toxicity and minimal side effects on the human body. In the future, to facilitate clinical applications, confocal systems with multiple excitation wavelengths might be developed in order to be suitable for the excitation of a wide range of fluorescent dyes. As fluorescent dyes can only be excited within a certain spectral range, it is inappropriate for us to use white light as light source [36, 37]. Compared with reflection endoscopy, confocal endoscopy with fluorescence could obtain more information about tissues.

The object of confocal endoscopy observations is typically epithelial cells. Cells are the basic structural and functional unit of an organism. Because confocal endoscopy achieves a higher magnification and resolution than conventional endoscopy, it permits clear observation of cells and holds the possibility of studying many types of cell activities *in vivo*. In this way, cell activities in real time would be better understood and an accurate diagnosis could be made in the early stage of a disease, which is currently difficult to achieve because cells function quite differently under healthy versus pathological conditions.

In summary, we have presented a confocal endoscope system based on a flexible fiber bundle with high resolution and contrast. The high resolution and wide field of the system were tested using the USAF target and a standard grating and were further demonstrated by experiments on mice. The confocal endoscope is a unique tool for understanding microstructures on the surface of tissue. The images from mice exhibited fundamental structures of the colon. The small size of the probe makes it possible for use in clinical applications with the help of a conventional endoscope, which will be helpful in avoiding repeated biopsies during endoscopy and in enabling the early diagnosis of diseases in the digestive tract.

Acknowledgements

The authors thank Hui Li, Nian Tian, Zhou Zhou, and Geng Tian for image analysis and Ying Wang for providing information related to the fiber scanning devices. The authors also greatly appreciate Xiu Nie from the Department of Pathology of Union Hospital at Huazhong University of Science and Technology for help with the histologic specimen. This work was supported by the National Key Technology R&D Program of China (2011BAI12B06), and National Natural Science Foundation of China (61205197 and 61178077).

Compliance with ethics guidelines

Jiafu Wang, Min Yang, Li Yang, Yun Zhang, Jing Yuan, Qian Liu, Xiaohua Hou, and Ling Fu declare that they have no conflict of interest or financial conflicts to disclose.

References

1. B. Stewart, C. P. Wild. *World Cancer Report 2014*. Geneva: World Health Organization, 2014
2. T. A. Stamey, N. Yang, A. R. Hay, J. E. McNeal, F. S. Freiha, E. Redwine. Prostate-specific antigen as a serum marker for adenocarcinoma of the

prostate. *N. Engl. J. Med.*, 1987, 317(15): 909–916
3. J. M. Edmonson. History of the instruments for gastrointestinal endoscopy. *Gastrointest. Endosc.*, 1991, 37(Suppl. 2): S27–S56
4. B. I. Hirschowitz, C. W. Peters, L. E. Curtiss. Preliminary report on a long fiberscope for examination of stomach and duodenum. *Med. Bull. (Ann Arbor)*, 1957, 23(5): 178–180
5. B. I. Hirschowitz. A personal history of the fiberscope. *Gastroenterology*, 1979, 76(4): 864–869
6. J. Pohl, et al. Comparison of computed virtual chromoendoscopy and conventional chromoendoscopy with acetic acid for detection of neoplasia in Barrett's esophagus. *Endoscopy*, 2007, 39(7): 594–598
7. ASGE Technology Committee; L. M. Wong Kee Song, et al. Chromoendoscopy. *Gastrointest. Endosc.*, 2007, 66(4): 639–649
8. K. K. Wang, N. Okoro, G. Prasad, M. Wong Kee Song, N. S. Buttar, J. Tian. Endoscopic evaluation and advanced imaging of Barrett's esophagus. *Gastrointest. Endosc. Clin. N. Am.*, 2011, 21(1): 39–51
9. R. Kiesslich, et al. Confocal laser endoscopy for diagnosing intraepithelial neoplasias and colorectal cancer *in vivo*. *Gastroenterology*, 2004, 127(3): 706–713
10. M. Goetz, N. P. Malek, R. Kiesslich. Microscopic imaging in endoscopy: Endomicroscopy and endocytoscopy. *Nat. Rev. Gastroenterol. Hepatol.*, 2014, 11(1): 11–18
11. A. Meining, et al. Direct visualization of indeterminate pancreaticobiliary strictures with probe-based confocal laser endomicroscopy: A multicenter experience. *Gastrointest. Endosc.*, 2011, 74(5): 961–968
12. T. Liu, H. Zheng, W. Gong, C. Chen, B. Jiang. The accuracy of confocal laser endomicroscopy, narrow band imaging, and chromoendoscopy for the detection of atrophic gastritis. *J. Clin. Gastroenterol.*, 2015, 49(5): 379–386
13. M. Goetz. Endomicroscopy and targeted imaging of gastric neoplasia. *Gastrointest. Endosc. Clin. N. Am.*, 2013, 23(3): 597–606
14. L. Ginlünas, R. Juškaitis, S. V. Shatalin. Scanning fibre-optic microscope. *Electron. Lett.*, 1991, 27(9): 724–726
15. M. Gu, C. J. R. Sheppard, X. Gan. Image formation in a fiber-optical confocal scanning microscope. *J. Opt. Soc. Am. A*, 1991, 8(11): 1755–1761
16. S. Kimura, T. Wilson. Confocal scanning optical microscope using single-mode fiber for signal detection. *Appl. Opt.*, 1991, 30(16): 2143–2150
17. A. F. Gmitro, D. Aziz. Confocal microscopy through a fiber-optic imaging bundle. *Opt. Lett.*, 1993, 18(8): 565–567
18. M. B. Wallace, P. Fockens. Probe-based confocal laser endomicroscopy. *Gastroenterology*, 2009, 136(5): 1509–1513
19. R. Kiesslich, M. Goetz, M. Vieth, P. R. Galle, M. F. Neurath. Technology insight: Confocal laser endoscopy for *in vivo* diagnosis of colorectal cancer. *Nat. Clin. Pract. Oncol.*, 2007, 4(8): 480–490
20. M. Goetz, A. Watson, R. Kiesslich. Confocal laser endomicroscopy in gastrointestinal diseases. *J. Biophotonics*, 2011, 4(7–8): 498–508
21. J. Knittel, L. Schnieder, G. Buess, B. Messerschmidt, T. Possner. Endoscope-compatible confocal microscope using a gradient index-lens system. *Opt. Commun.*, 2001, 188(5–6): 267–273
22. J. C. Jung, M. J. Schnitzer. Multiphoton endoscopy. *Opt. Lett.*, 2003, 28(11): 902–904
23. A. R. Rouse, A. Kano, J. A. Udovich, S. M. Kroto, A. F. Gmitro. Design and demonstration of a miniature catheter for a confocal microendoscope. *Appl. Opt.*, 2004, 43(31): 5763–5771
24. C. Liang, K. B. Sung, R. R. Richards-Kortum, M. R. Descour. Design of a high-numerical-aperture miniature microscope objective for an endoscopic fiber confocal reflectance microscope. *Appl. Opt.*, 2002, 41(22): 4603–4610
25. M. D. Chidley, K. D. Carlson, R. R. Richards-Kortum, M. R. Descour. Design, assembly, and optical bench testing of a high-numerical-aperture miniature injection-molded objective for fiber-optic confocal reflectance microscopy. *Appl. Opt.*, 2006, 45(11): 2545–2554
26. R. T. Kester, T. Christenson, R. R. Kortum, T. S. Tkaczyk. Low cost, high performance, self-aligning miniature optical systems. *Appl. Opt.*, 2009, 48(18): 3375–3384
27. M. Kyrish, et al. Needle-based fluorescence endomicroscopy via structured illumination with a plastic, achromatic objective. *J. Biomed. Opt.*, 2013, 18(9): 096003
28. W. Piyawattanametha, et al. *In vivo* brain imaging using a portable 2.9 g two-photon microscope based on a microelectromechanical systems scanning mirror. *Opt. Lett.*, 2009, 34(15): 2309–2311
29. J. Sawinski, D. J. Wallace, D. S. Greenberg, S. Grossmann, W. Denk, J. N. Kerr. Visually evoked activity in cortical cells imaged in freely moving animals. *Proc. Natl. Acad. Sci. U.S.A.*, 2009, 106(46): 19557–19562
30. J. Sawinski, W. Denk. Miniature random-access fiber scanner for *in vivo* multiphoton imaging. *J. Appl. Phys.*, 2007, 102(3): 034701
31. Y. Zhang, et al. A compact fiber-optic SHG scanning endomicroscope and its application to visualize cervical remodeling during pregnancy. *Proc. Natl. Acad. Sci. U.S.A.*, 2012, 109(32): 12878–12883
32. C. M. Lee, C. J. Engelbrecht, T. D. Soper, F. Helmchen, E. J. Seibel. Scanning fiber endoscopy with highly flexible, 1 mm catheterscopes for wide-field, full-color imaging. *J. Biophotonics*, 2010, 3(5–6): 385–407
33. B. A. Flusberg, E. D. Cocker, W. Piyawattanametha, J. C. Jung, E. L. M. Cheung, M. J. Schnitzer. Fiber-optic fluorescence imaging. *Nat. Methods*, 2005, 2(12): 941–950
34. Z. Li, Z. Yang, L. Fu. Scanning properties of a resonant fiber-optic piezoelectric scanner. *Rev. Sci. Instrum.*, 2011, 82(12): 123707
35. Z. Li, L. Fu. Note: A resonant fiber-optic piezoelectric scanner achieves a raster pattern by combining two distinct resonances. *Rev. Sci. Instrum.*, 2012, 83(8): 086102
36. R. Sjöback, J. Nygren, M. Kubista. Absorption and fluorescence properties of fluorescein. *Spectrochim. Acta A Mol. Biomol. Spectrosc.*, 1995, 51(6): L7–L21
37. V. K. Sharma, P. D. Sahare, R. C. Rastogi, S. K. Ghoshal, D. Mohan. Excited state characteristics of acridine dyes: Acriflavine and acridine orange. *Spectrochim. Acta A Mol. Biomol. Spectrosc.*, 2003, 59(8): 1799–1804
38. A. L. Polglase, W. J. McLaren, S. A. Skinner, R. Kiesslich, M. F. Neurath, P. M. Delaney. A fluorescence confocal endomicroscope for *in vivo* microscopy of the upper- and the lower-GI tract. *Gastrointest. Endosc.*, 2005, 62(5): 686–695
39. J. M. Jabbour, M. A. Saldua, J. N. Bixler, K. C. Maitland. Confocal endomicroscopy: Instrumentation and medical applications. *Ann. Biomed. Eng.*, 2012, 40(2): 378–397
40. S. C. Park, M. K. Park, M. G. Kang. Super-resolution image reconstruction: A technical overview. *IEEE Signal Proc. Mag.*, 2003, 20(3): 21–36
41. S. Lertrattanapanich, N. K. Bose. High resolution image formation from low resolution frames using Delaunay triangulation. *IEEE Trans. Image Process.*, 2002, 11(12): 1427–1441
42. T. Kuiper, et al. New classification for probe-based confocal laser endomicroscopy in the colon. *Endoscopy*, 2011, 43(12): 1076–1081
43. M. Goetz, et al. *In vivo* molecular imaging of colorectal cancer with confocal endomicroscopy by targeting epidermal growth factor receptor. *Gastroenterology*, 2010, 138(2): 435–446
44. D. Moussata, et al. Confocal laser endomicroscopy is a new imaging modality for recognition of intramucosal bacteria in inflammatory bowel disease *in vivo*. *Gut*, 2011, 60(1): 26–33
45. Y. Goto, H. Kiyono. Epithelial barrier: An interface for the cross-communication between gut flora and immune system. *Immunol. Rev.*, 2012, 245(1): 147–163
46. S. Foersch, et al. Molecular imaging of VEGF in gastrointestinal cancer *in vivo* using confocal laser endomicroscopy. *Gut*, 2010, 59(8): 1046–1055